Energy and Density Analyses of the $^1\Sigma_u^+$ States in the H_2 Molecule from the United Atom to Dissociation[†]

Giorgina Corongiu*

Dipartimento di Scienze Chimiche e Ambientali, Università dell'Insubria,
Via Valleggio 11, I-22100 Como, Italy

Enrico Clementi

Via Carloni, 38, I-22100 Como, Italy

Received: May 27, 2009; Revised Manuscript Received: July 7, 2009

The $^1\Sigma_u^+$ excited states of the H_2 molecule are computed following a recent study by Corongiu and Clementi (*J. Chem. Phys.* **2009**, *131*, 034301) on the $^1\Sigma_g^+$ states. Full configuration interaction computations both from Hartree–Fock molecular orbitals and Heitler–London atomic orbitals are presented and correlated with a comprehensive analysis. The basis sets utilized are either extended and optimized Slater type functions, STO, or spherical Gaussian functions, GTO. Computations and analyses are presented for states 1 to 14, covering the internuclear distances from 0.01 to 10000 bohr. The accurate data by L. Wolniewicz and collaborators, available for the first six excited states, verify the good quality of our computations. We focus on the characterization of the orbitals in the excited state wave functions, on the electronic density evolution from the united atom to dissociation, on quantitative decomposition of the total energy into covalent and ionic components and on detailed analyses of energy contributions to the total state energy from selected STO subsets. Each manifold has one state, specifically the states 1, 3 and 6, where the second minimum has strong ionic character. State 10 dissociates into the ion pair H^+H^-.

1. Introduction

This work reports computations of the $^1\Sigma_u^+$ excited states 1 to 14 for the H_2 molecule, following a computational approach recently proposed[1] for a study on the $^1\Sigma_g^+$ excited states. Energies of the united atom and dissociation products, discussions on the choice of the basis sets, details on the techniques used to analyze the obtained wave functions and energies when in common both to this work and to ref 1 are here only summarized.

The $^1\Sigma_u^+$ excited states have been often studied.[2–9] The most accurate potential energy curves, PECs, for the first six states are those by Staszewska and Wolniewicz.[9] Accurate computations for the first 9 states, using generalized Gaussian functions, have been published by Cederbaum et al.,[7] where, however, the PECs for the states are mainly reported only graphically.

In Figure 1 the state orbital diagram for the $^1\Sigma_u^+$ excited state manifolds reports the electronic states for the united atom (He), the dissociation products for the H_2 molecule up to $n = 4$, i.e. H(1s) + H(4l), the lowest state energy for the $H_2{}^+$ molecular ion and the lowest state energy for the H^+H^- system.[1] At the left side of Figure 1 we report the excited state energies for helium (the united atom), the corresponding designations (1 to 9) of the molecular excited states and state connections from the united atom to the H_2 atomic dissociation products, namely the two atoms H(1s) and H(nl), indicated in the figure with the short notation $n = 2$, 3, and 4. The l value varies from 0 to 3 (i.e., from s to f orbitals) corresponding to the excited states 1B to 9B, namely up to $n = 4$. Note that the last helium state (1s7p) is not connected to the right site of the diagram, since the dissociation products for $n = 5$ are not reported. The computations include also states with dissociation $n = 5$, not indicated in Figure 1.

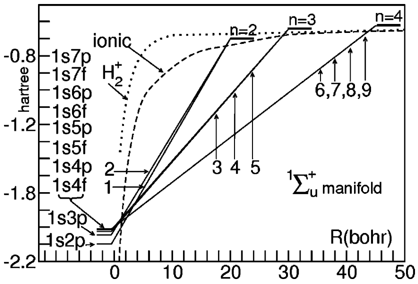

Figure 1. State diagram for the $^1\Sigma_u^+$ excited states 1 to 9 of the H_2 molecule.

In the following of this work we use both the full state notation nB with $n = 1, ..., 9$, or simply the shorthand designation 1, ..., 9, as done in the figure, to denote different $^1\Sigma_u^+$ states. Computationally, these high states require very extended basis sets capable of describing from He(1s2p) up to He($1s^19p^1$) and He($1s^19f^1$) at the united atom and from H(1s) up to H(5l), with l up to 4, at dissociation; for this reason states 10B to 14B are considered rather briefly and the corresponding computations are somewhat less reliable, being obtained with nonoptimal basis sets.

2. The $^1\Sigma_u^+$ Excited States

The computations of the PECs start at the united atom and end at the internuclear distance of 10^4 bohr. Two extended basis sets are used in this study: one constructed with exponential functions of Slater type, STO, the second with spherical Gaussian functions, GTO. These optimized basis sets are nearly

---

[†] Part of the "Vincenzo Aquilanti Festschrift".

10.1021/jp9049395

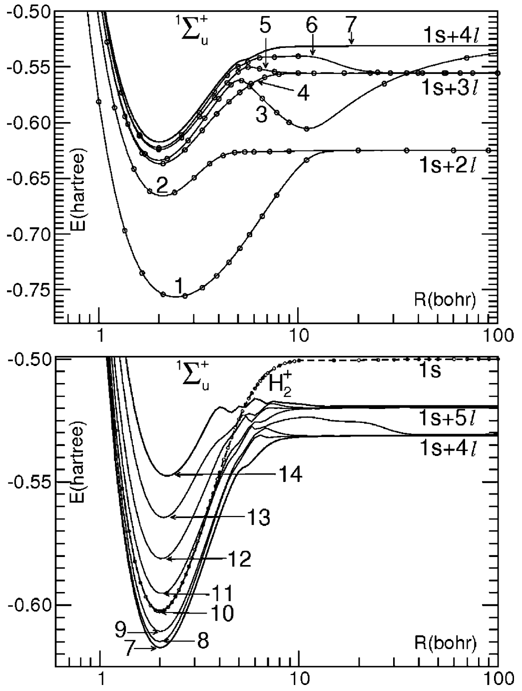

Figure 2. PECs for the $^1\Sigma_u^+$ excited states of the H_2 molecule.

equivalent, and the computations obtained with the two types of functions yield slightly different eigenvalues (and corresponding slightly different electronic densities) for a given internuclear separation. The use of two different functions, STO and GTO, provides a useful numerical check and adds flexibility to the interpretation of the computations, as discussed in ref 1.

The STO basis set is made of two 1s, three 2s, two 3s, one 4s, one 5s, four 2p, two 3p, one 4p, one 5p, four 3d, one 4d, one 5d, three 4f, and two 5f functions. The GTO basis set is made of 17s,10p,11d, 7f contracted to 12s, 10p, 8d and 5f. At the united atom the helium basis set is formed by three 1s, three 2s, two 3s, two 4s, one 5s, two 6s, four 2p, two 3p, two 4p, two 5p, one 6p, four 3d, one 4d, two 5d, one 6d, four 4f, three 5f and one 6f functions. With this basis set we well represent the energies of the helium singly excited states with configuration up to (1s6f). The dissociation products are well represented by the STO basis set, which accurately reproduces hydrogenic functions: in this study the hydrogenic functions have *nl* values ranging from $n = 1$ to $n = 5$ and $l = 0$ to $l = 3$; additional details on the hydrogenic functions for H_2 are given in ref 1.

In Figure 2 the computed PECs for the $^1\Sigma_u^+$ excited states 1B to 14B are reported. The internuclear separations considered in the computations are 130, precisely 25 from 0.01 to 1.0 bohr, 105 from 1.0 to 100 bohr; computations at 1000 and 10000 bohr are performed to define the dissociation products. In the top panel the PECs of the first 7 states are reported. In this figure the small circles represent a selected sample of energies from Wolniewicz data.[9] In the bottom panel the PECs for states 7 to 14 and for H_2^+ are reported. The PECs for the states dissociating into H(1s) + H(4*l*) are computed more accurately than those for the states dissociating into H(1s) + H(5*l*), therefore the latter are considered mainly to complete the $^1\Sigma_u^+$ state survey.

Note for state 3B the avoided crossing with state 4B at about 5.7 bohr, and its second deep minimum at ~11 bohr. State 6B has a shallow second minimum leading to the 1s + 4*l* dissociation limit after 100 bohr. State 7B shows a flexion point around 5.6 bohr. States 8B and 9B are nearly degenerate from about 3.5 to 4.5 bohr and show an avoided crossing at ~6.1 bohr. State 10B is very close in energy to the H_2^+ ground state (dashed line with circles) and from ~10 bohr starts a slow energy decrease leading to the H^+H^- dissociation limit. States 11B to 14B lie well above the PEC of H_2^+ (reported mainly to complete the $^1\Sigma_u^+$ state manifold).

The accuracy of the computed energies relative to those of Wolniewicz is evident from Figure 2. Numerically, the average deviations (in hartree) are 1.3×10^{-4} (with maximum deviation of 2.3×10^{-4} at 4.1 bohr), 2.0×10^{-5} (with maximum deviation of 5.6×10^{-5} at 1.8 bohr), 7.2×10^{-5} (with maximum deviation of 1.9×10^{-4} at 14 bohr), 2.3×10^{-5} (with maximum deviation of 1.1×10^{-4} at 5.5 bohr), 2.9×10^{-5} (with maximum deviation of 4.0×10^{-4} at 1.1 bohr), 9.6×10^{-5} (with maximum deviation of 2.0×10^{-4} at 1.8 bohr), for states 1 to 6, respectively. In the first three columns of Table 1 we compare for each state the computed energy near the minimum positions with the data from ref 9. In the fourth and fifth columns of Table 1 we report the computed equilibrium distance and the corresponding energy. In the last two columns we report the laboratory data.[10] For states 7B to 12B at 2.0 bohr and for states 13B and 14B at 2.1 bohr the energies (in hartree) are −0.61741, −0.61493, −0.61077, −0.60249, −0.59530, −0.58116, −0.56447, and −0.54754, respectively. The finding that the minimum of states 11 to 14 is above the H_2^+ ion energy might be due to the basis set difficulty to well represent these high states. Addition of one 5g function improves the energy of the last four states to −0.59684, −0.59579, −0.57962, and −0.56390. With the same basis set we obtain for the $1\sigma_g$ and $1\sigma_u$ states of the H_2^+ ion, at 2.0 bohr, the energies of −0.602633 and −0.167533 hartree, respectively; both values differ by 1.5×10^{-6} hartree from the best results of ref 11.

For very short internuclear distances we report the computed results in Figure 3. The PECs of this figure correspond to electronic rather than total energies, for graphical reasons. The PECs of the top panel accurately merge into the expected helium excited state energies, as shown in the figure. From $R = 0.01$ to 0.1 bohr the PECs are obtained from computations with the helium STO basis set centered midway the two hydrogen nuclei. From 0.1 to 0.9 bohr, the PECs are more accurately obtained with the GTO basis set centered on the hydrogen nuclei.

In literature the PECs at short distances are often approximated with linear interpolation from the helium atomic energies with those computed at distances near 1.0 bohr. The data from Figure 3 indicate that the linear interpolation is reasonable until about 0.3 bohr; at shorter distances deviations from linearity are noted.

For the first 10 states (with energy at the minimum below the H_2^+ ion energy) a tabulation of the computed energies at selected internuclear distances is provided in Table 2; from $R = 0$ to $R = 0.6$ bohr we have reported the electronic energy, thereafter the total energy.

3. Decomposition into Ionic and Covalent Components

The full-CI of HL orbitals facilitates the decomposition of the total state energies into ionic and covalent components.[1] In the top panel of Figure 4 we report for states 1B to 7B both the total energy and the corresponding covalent component. The covalent component for states 1B, from ~2.2 bohr until dissociation, and for states 3B, and 6B, in the region of their second minimum, is clearly in need of the ionic component.

The state energies for the system H^+H^- are reported (bullets) in the bottom panel of Figure 4. The states are very near in

TABLE 1: Comparison of Total Energies, E (hartree), near the Minimum Positions, R (bohr), from Wolniewicz Data[9] and from this Work; Computed Equilibrium Distance, R_{eq} (bohr), and Energy, E_{eq} (hartree), from this Work[a]

		$-E$					
state	R	ref 9	this work	R_{eq}	$-E_{eq}$	R(exp)	$-E$(exp)
1B	2.4	0.756674	0.75652	2.420	0.75653	2.4431	0.756660
2B	2.1	0.665791	0.66576	2.085	0.66577	2.1150	0.665793
3B	2.0	0.636960	0.63695	2.032	0.63698	2.1161	0.636899
3B	11.1	0.605666	0.60551	11.12	0.60551		
4B	2.0	0.634102	0.63409	2.000	0.63409		
5B	2.0	0.624204	0.62419	2.012	0.62419		
6B	2.0	0.622749	0.62271	1.998	0.62272		
6B	34.0	0.555504	0.55548	33.80	0.55548		

[a] The last two columns, R(exp) and E(exp), are laboratory data.[10]

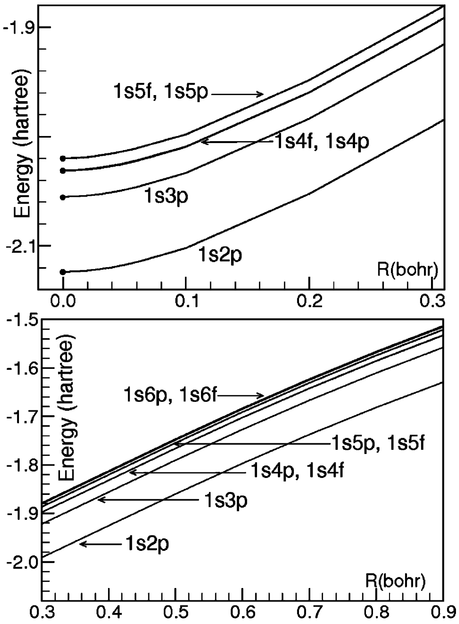

Figure 3. Short distance electronic energies. Top: from the united atom ($R = 0$) to 0.3 bohr. Bottom: from 0.3 to 0.9 bohr.

energy to those of H_2 (solid lines), but slightly at higher energy from short to intermediate distances. The difference between the H_2 and H^+H^- energies is notable mainly after the first minimum toward large internuclear distances, around 4−5 bohr, where the H^+H^- states are experimentally detected.[12] In this panel we report also the H^+H^- curve computed with the analytic expression of ref 7, this curve (dashed line) overlaps that of the H^+H^- ground state and that of state 6B from 12 bohr until dissociation, for shorter internuclear distances it is much less attractive. Indeed, from 10 to 12 bohr it overlaps with the curve of state 2B, whereas we find that it is the second excited state of H^+H^- which overlaps state 2B.

As demonstrated by Slater,[13] for the H_2 molecule the HL covalent and ionic functions, though orthogonal at infinity, are highly nonorthogonal at equilibrium and at shorter distances, actually the shorter the internuclear distance the more the two functions resemble one another. This is not surprising since the two functions must become identical at the united atom. Further, as pointed out by Mulliken,[14] although the excited ionic states are only virtual states for internuclear distances approaching infinity, at small and intermediate distances the stabilization induced by H^+ on the excited H^- should convert the virtual states into real states. Indeed, from Figure 4 it is evident that for large internuclear distances the PECs of the excited H^+H^- states are above the dissociation limit, and therefore unstable.

Following the H_2 study of ref 1, we define the quantity η as the ratio between the covalent energy component and the total energy, $\eta = E(\text{covalent})/E(\text{total})$. This leads to the definition of the ionic energy percent, IEP = $100(1 - \eta)$ also introduced in ref 1. Figure 5 reports the IEP for the $^1\Sigma_u^+$ states, in the top panel for the states 1B, 3B and 6B and in the bottom panel for states 2B, 4B, and 5B. Note that for the latter three states the IEP is very small and localized, with sharp variations due to state interactions and state crossing. In addition, whereas for states 3B and 6B the maximum of IEP occurs at the second minimum position, for state 1B we see an almost constant contribution from 5 to 8 bohr. The second minimum of state 3B has been experimentally observed,[12,15] whereas that of state 6B has only been found from computations.[7,9] However, unresolved H^+H^- states above the $n = 4$ threshold were shown to exist by wave-packets experiments.[16]

For the $^1\Sigma_g^+$ states it has been found[1] that for each state manifold dissociating as (1snl) with $n > 1$ there is one state which interacts with the H^+H^- system leading to minima at larger and larger internuclear separations the higher the value of n. Indeed, a strong ionic character for states EF, H, 7, and 11 was observed. This finding is here extended to the $^1\Sigma_u^+$ state manifolds, the states 1B, 3B, 6B and 10B, all with ionic character, have dissociation limits (1s2p), (1s3d), (1s4d) and the ion pair H^+H^-, respectively.

By grouping together states with the same n value in the dissociation products H(1s) + H(nl), we obtain the four panels of Figure 6. For each n value we report the H_2 states of $^1\Sigma_g^+$ symmetry (see ref 1), those of $^1\Sigma_u^+$ symmetry, and those of the H^+H^- system (see ref 1). The panels of the figure are complicated because of small energy differences between states; the figure reveals simply by inspection the complexity of these "simple" molecular systems. To facilitate the reading of the figure only a few states are explicitly identified; for example the labels 1g and 1u refer to the first excited state of symmetry g and u, respectively.

4. Electronic Density Analysis

In this section we analyze for each state its orbital composition at specified internuclear distances, using an analysis based on the H_2 wave functions—obtained with the STO basis sets—equivalent to the atomic radial distribution function, $D_{nl}(r)$; the details of this comparative analysis are available in ref 1.

Since the density in the H_2 molecule is symmetric upon reflection in the plane perpendicular to the midpoint of the molecular axis (z axis), and for any given internuclear distance the molecular orbitals are linear combinations of STO basis functions centered at the two nuclear positions, it follows that the knowledge of the STO linear combination at one nuclear position characterizes the electronic density also at the other nuclear position. Further for a given state and for a given

TABLE 2: Energy Values (hartree) at Internuclear Distances, *R* (bohr), for States 1 to 10

no.	0.00	0.01	0.02	0.20	0.40	0.60	0.80	1.00	1.20	1.40	1.60
1	−2.12376	−2.12350	−2.12272	−2.05257	−1.92533	−1.79716	−0.43179	−0.58129	−0.66127	−0.70570	−0.73069
2	−2.05512	−2.05485	−2.05408	−1.98377	−1.85610	−1.72716	−0.36064	−0.50861	−0.58663	−0.62867	−0.65084
3	−2.03125	−2.03099	−2.03021	−1.95983	−1.83199	−1.70277	−0.33598	−0.48357	−0.56111	−0.60256	−0.62403
4	−2.03101	−2.03075	−2.02997	−1.95967	−1.83189	−1.70275	−0.33576	−0.48309	−0.56030	−0.60133	−0.62232
5	−2.02000	−2.01974	−2.01896	−1.94855	−1.82070	−1.69149	−0.32460	−0.47205	−0.54942	−0.59066	−0.61187
6	−2.01982	−2.01955	−2.01878	−1.94849	−1.82068	−1.69145	−0.32446	−0.47178	−0.54898	−0.59000	−0.61097
7	−2.01317	−2.01290	−2.01213	−1.94233	−1.81451	−1.68530	−0.31836	−0.46577	−0.54307	−0.58422	−0.60534
8	−2.00991	−2.00965	−2.00887	−1.94070	−1.81289	−1.68366	−0.31667	−0.46399	−0.54119	−0.58222	−0.60319
9	−1.98096	−1.98069	−1.97991	−1.93465	−1.80683	−1.67764	−0.31078	−0.45829	−0.53573	−0.57705	−0.59834
10	−1.96187	−1.96160	−1.97604	−1.92796	−1.80017	−1.67096	−0.30398	−0.45131	−0.52854	−0.56960	−0.59062

no.	1.70	1.90	2.00	2.10	2.20	2.40	2.80	3.00	3.20	3.60	4.00
1	−0.73867	−0.74888	−0.75196	−0.75408	−0.75544	−0.75652	−0.75456	−0.75234	−0.74957	−0.74291	−0.73526
2	−0.65727	−0.66414	−0.66545	−0.66576	−0.66530	−0.66274	−0.65425	−0.64946	−0.64481	−0.63680	−0.63129
3	−0.63007	−0.63609	−0.63695	−0.63679	−0.63584	−0.63227	−0.62163	−0.61570	−0.60983	−0.59906	−0.59014
4	−0.62810	−0.63354	−0.63409	−0.63362	−0.63235	−0.62812	−0.61605	−0.60935	−0.60263	−0.58987	−0.57869
5	−0.61778	−0.62350	−0.62419	−0.62387	−0.62275	−0.61882	−0.60741	−0.60106	−0.59473	−0.58288	−0.57269
6	−0.61674	−0.62217	−0.62271	−0.62223	−0.62094	−0.61669	−0.60457	−0.59782	−0.59106	−0.57818	−0.56684
7	−0.61119	−0.61678	−0.61741	−0.61701	−0.61582	−0.61174	−0.60000	−0.59345	−0.58691	−0.57457	−0.56381
8	−0.60896	−0.61439	−0.61493	−0.61444	−0.61316	−0.60890	−0.59676	−0.59001	−0.58325	−0.57038	−0.55907
9	−0.60427	−0.61005	−0.61077	−0.61046	−0.60935	−0.60544	−0.59398	−0.58756	−0.58114	−0.56898	−0.55829
10	−0.59642	−0.60191	−0.60249	−0.60204	−0.60079	−0.59663	−0.58473	−0.57812	−0.57151	−0.55911	−0.54933

no.	4.40	4.80	5.20	5.60	5.80	6.40	7.00	7.60	8.00	9.00	10.00
1	−0.72711	−0.71877	−0.71048	−0.70240	−0.69848	−0.68729	−0.67706	−0.66783	−0.66222	−0.65011	−0.64054
2	−0.62826	−0.62692	−0.62644	−0.62630	−0.62628	−0.62621	−0.62610	−0.62596	−0.62586	−0.62565	−0.62548
3	−0.58289	−0.57681	−0.57168	−0.56781	−0.56869	−0.57593	−0.58290	−0.58907	−0.59266	−0.59965	−0.60390
4	−0.56961	−0.56344	−0.56231	−0.56547	−0.56517	−0.56119	−0.55863	−0.55724	−0.55672	−0.55612	−0.55589
5	−0.56422	−0.55734	−0.55240	−0.55023	−0.55025	−0.55177	−0.55321	−0.55420	−0.55465	−0.55529	−0.55552
6	−0.55753	−0.55132	−0.54858	−0.54572	−0.54447	−0.54194	−0.54127	−0.54122	−0.54113	−0.54066	−0.54036
7	−0.55484	−0.54796	−0.54436	−0.54293	−0.54171	−0.53782	−0.53509	−0.53348	−0.53282	−0.53201	−0.53170
8	−0.54995	−0.54416	−0.53965	−0.53541	−0.53358	−0.53097	−0.53187	−0.53173	−0.53158	−0.53145	−0.53141
9	−0.54928	−0.54240	−0.53847	−0.53439	−0.53247	−0.52928	−0.52841	−0.52957	−0.53010	−0.53087	−0.53115
10	−0.54239	−0.53826	−0.53349	−0.52888	−0.52734	−0.52807	−0.52689	−0.52576	−0.52532	−0.52432	−0.52380

no.	11.00	11.10	12.00	13.00	20.00	30.00	34.00	40.00	50.00	100	10000
1	−0.63358	−0.63303	−0.62921	−0.62697	−0.62514	−0.62504	−0.62503	−0.62502	−0.62501	−0.62500	−0.62500
2	−0.62536	−0.62535	−0.62527	−0.62519	−0.62500	−0.62500	−0.62500	−0.62500	−0.62500	−0.62500	−0.62500
3	−0.60549	−0.60551	−0.60461	−0.60187	−0.57827	−0.56109	−0.55711	−0.55556	−0.55555	−0.55555	−0.55555
4	−0.55578	−0.55578	−0.55572	−0.55567	−0.55557	−0.55555	−0.55555	−0.55554	−0.55554	−0.55554	−0.55554
5	−0.55559	−0.55559	−0.55559	−0.55558	−0.55554	−0.55553	−0.55553	−0.55553	−0.55553	−0.55552	−0.55552
6	−0.54048	−0.54053	−0.54118	−0.54244	−0.55281	−0.55542	−0.55548	−0.55261	−0.54758	−0.53756	−0.53122
7	−0.53159	−0.53158	−0.53153	−0.53147	−0.53126	−0.53122	−0.53122	−0.53121	−0.53122	−0.53122	−0.53120
8	−0.53138	−0.53137	−0.53134	−0.53131	−0.53120	−0.53117	−0.53117	−0.53118	−0.53120	−0.53120	−0.53114
9	−0.53124	−0.53124	−0.53124	−0.53123	−0.53117	−0.53104	−0.53104	−0.53111	−0.53115	−0.53114	−0.53056
10	−0.52361	−0.52362	−0.52382	−0.52432	−0.52559	−0.52934	−0.53030	−0.53074	−0.53069	−0.53058	−0.52766

internuclear distance, *R*, the STO linear combination generally is characterized by relatively few dominant STO functions.

Recall that the radial distribution function for an atom with wave function $\psi(r,\theta,\varphi)$ is $D_{nl}(r) = \psi^2(r)r^2$.[17] We introduce a molecular function devised to represent the radial distribution function of an atom in a molecule. Specifically for H_2 we consider the electronic density centered on one of the H atoms, set at the origin of the coordinate system (the other atom being at $z = -R$). For a given *state* of H_2 and at a given internuclear distance, *R*, we compute $\psi^2(0,0,z)z^2$ for a set of *z* values, in the interval 0 to infinity. In analogy with the atomic computations of $D_{nl}(r)$, we consider the function $\psi^2(0,0,z)z^2$ as a probability distribution function along the *z* axis for that H atom in H_2. The function is characteristic for a given state and for a given *R* value, and for H_2 is designated as $D_{\text{state}}(1s,nl)$ or simply "*state*"(1s,*nl*). Clearly at $R = 0$, the D_{nl}(r) for a given helium state coincides with "*state*"(1s,*nl*).

As reported in ref 1, the $D_{nl}(r)$s for H^- are notably different from those of the H or He atoms and resemble the 1s radial distribution, but with a density nearly nodeless and with a slow decaying toward zero density at large *r* values.

In the left panels of Figure 7 we report the plots obtained by adding $D_{1s}(r)$ to $D_{nl}(r)$ of hydrogenic functions. These composed distributions are taken as "reference distributions" for the dissociation products H(1s) + H(*nl*). In Figure 7 (right panels) we report the "*state*"(1s,*nl*) obtained from computations with the STO basis set at the internuclear distance of 10000 bohr, i.e. at dissociation. Each plot of the radial distribution functions relates to two orbitals: the 1s orbital generates a peak at very short distance, and the *nl* orbital, with $n = 2$ to 5 and $l = 0$ to 3, yields the distribution located at variable distances.

In the figure we compare the number of nodes and the positions of the corresponding maxima (not the intensities) of the $D_{nl}(r)$ at infinite separation, with those computed at the internuclear distance $R = 10000$ bohr; for example, the distribution 6(1s3d) in the left top panel has its counterpart in the distribution 3(1s3d) in the right top panel. From this comparison, keeping in mind that one hydrogen orbital is always of 1s type, one can identify the distribution for the other orbital, namely the orbitals 2p, 2s, 3d, 3p, 3s, 4d, 4f, 4s, 4p, ionic, designated (1s′1s′), 5d, 5s, 5p and 5f, characterizing the states

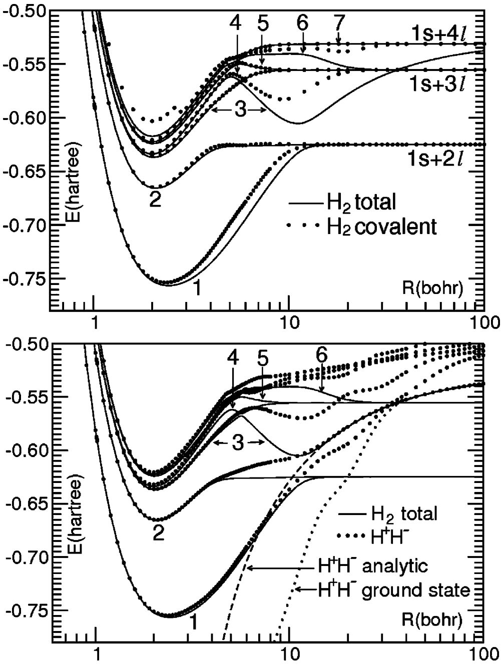

Figure 4. Top: total and corresponding covalent energy component for the states 1 to 7. Bottom: energies for the system H^+H^-.

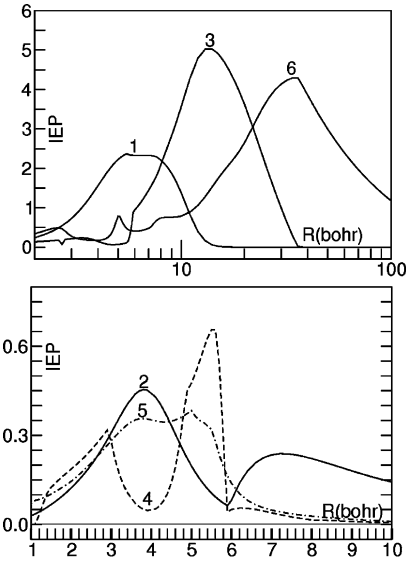

Figure 5. IEP for the $^1\Sigma_u^+$ states. Top: for 1B, 3B and 6B states. Bottom: for 2B, 4B, and 5B.

1B to 14B, respectively. This comparison relates to the computed dissociation products. Note that the hydrogenic distributions $D_{nl}(r)$ are generated orderly, i.e. state 2 corresponds to $n = 2$ and $l = 0$, state 3 to $n = 2$ and $l = 1$, etc., Further, state 1, $n = 1$ and $l = 0$, is omitted since no $^1\Sigma_u^+$ state dissociates as H(1s) + H(1s). For the computed distributions on the left panels, the sequence of the integers 1, 2, 3, ... represents the order of the roots obtained from the diagonalization of the secular equation, thus the state order is assigned unambiguously.

In Figure 8 we report the radial distribution functions for states 1B to 9B at the internuclear distances of 0.5 bohr (i.e., approaching the helium united atom) and 2.0 bohr, the distance near the first minimum for most states (see Table 1). The symmetry of the system imposes that at the united atom the state configurations are restricted to (1snp) and (1snf). In Figure 8 the radial distribution functions at 0.5 bohr respect this symmetry constraint. However, at the united atom, the states (1snp) and (1snf) are known to be nearly degenerate[18] with the energies of the states (1snf) slightly lower than those of the states (1snp). Computationally, we correctly obtain the two states very close in energy, but our hydrogen basis set yields the energy of the states (1snp) slightly lower than that of the states (1snf). Therefore, approaching the united atom state crossings, not detected by our computations, are expected between the pairs of states 3 and 4, 5 and 6, 7 and 9.

From the right panels of Figure 8, at the internuclear distance of 2.0 bohr, we see a variety of state configurations. The configuration of 1B is a mixture of the ionic (1s′1s′) with the (1s2p) configurations, then the configurations (1snp) at 0.5 bohr switch to (1snd) at 2.0 bohr.

We have computed the radial distribution functions for each state at 19 internuclear separations, starting at $R = 0.5$ bohr and ending at 100 bohr; the density at dissociation is analyzed twice, at $R = 1000$ and 10000 bohr, as for the $^1\Sigma_g^+$ states,[1] the two computations yield the same results.

The 1B state from dissociation to about 15 bohr has the electronic configuration (1s2p), which becomes ionic (1s′1s′) until 2.2 bohr, and at 2.0 it becomes a mixture of (1s′1s′) and (1s2p) until it merges into the united atom configuration He(1s2p). The relative importance of ionic and covalent components for this state has been discussed by Kolos[3] and Mulliken.[14] The electronic configurations at the united atom, at dissociation and at intermediate internuclear distances are in agreement with those proposed by Mulliken.[14]

The 2B state configuration from dissociation to about 5.0 bohr is (1s2s); from 2.5 bohr to 2.0 becomes (1s3d), then (1s3p) until it merges into He(1s3p). Again, this is in agreement with Mulliken.[14]

The state 3B configuration from dissociation to ∼100 bohr is (1s3d), and then it becomes the ionic configuration (1s′1s′) until 5.7 bohr where there is a mixture of the ionic and (1s2s) configurations. From 5.4 to 5.0 bohr it is (1s3p); from 2.5 to 2.0 bohr it becomes (1s4d) and from 1.0 to 0.5 bohr (1s4p) merging into the united atom He(1s4f).

The state 4B configuration from dissociation to 6.2 bohr is (1s3p). From 5.7 to 5.4 bohr it is a mixture of ionic and (1s3*l*) likely (1s3s); this is the region of an avoided state crossing with the 3B state. As shown in the bottom panel of Figure 4 the ionic state 3 of H^+H^- overlaps with state 4B between 5.4 and 6 bohr. At 5.0 bohr the 4B configuration is (1s3d) and from 2.5 to the united atom it becomes (1s4*l*) first 4d, until 2.0 bohr, then 4f in approaching the united atom, rather then (1s4p).

The state 5B configuration from dissociation to 6.2 bohr is (1s3s), from 5.7 to 5.0 bohr is (1s4d); then from 2.5 to 0.5 bohr it becomes (1s5*l*) first (1s5d) until 1.0 bohr, then (1s5p) rather than (1s5f), the united atom.

The state 6B configuration at infinity is (1s4d), but it becomes ionic from 100 to15 bohr; from 15 to 5.0 bohr is (1s3*l*) mainly (1s3s), and from 2.5 to the united atom it is (1s5f) rather than (1s5p), the united atom configuration.

The state 7B configuration at dissociation is (1s4f), but it becomes (1s4d) at 100 bohr, and (1s4f) from 34 bohr to 10 bohr, then (1s4p) from 6.2 to 5.7 bohr and (1s5f) at 5 bohr. From 2.5 bohr to the united atom the configuration is (1s6*l*), specifically (1s6d) until 2.0 and then (1s6p); the united atom is He(1s6f).

The state 8B configuration at dissociation is (1s4s); from 20 to 15 it is (1s4d), at 10 bohr it is (1s4s); from 6.2 to 5.4 bohr it is (1s5f), from 2.5 to the united atom it becomes (1s6*l*) mainly (1s6f); the united atom is He(1s6p).

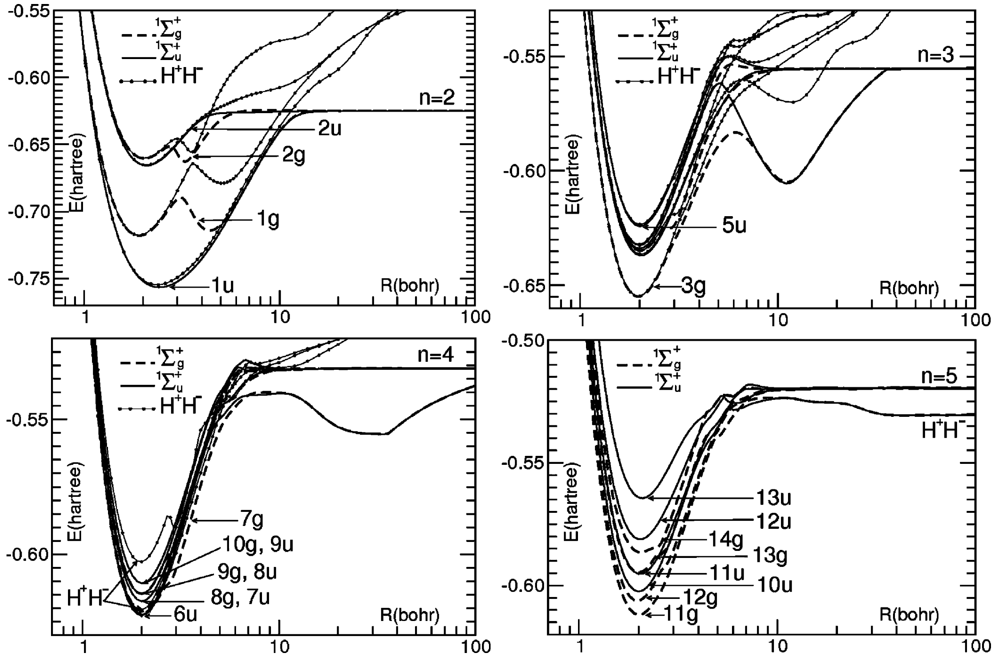

Figure 6. PECs for the $^1\Sigma_g^+$ states (dashed lines), $^1\Sigma_u^+$ states (full lines) in the H_2 molecule, and for the H^+H^- (full line with bullets).

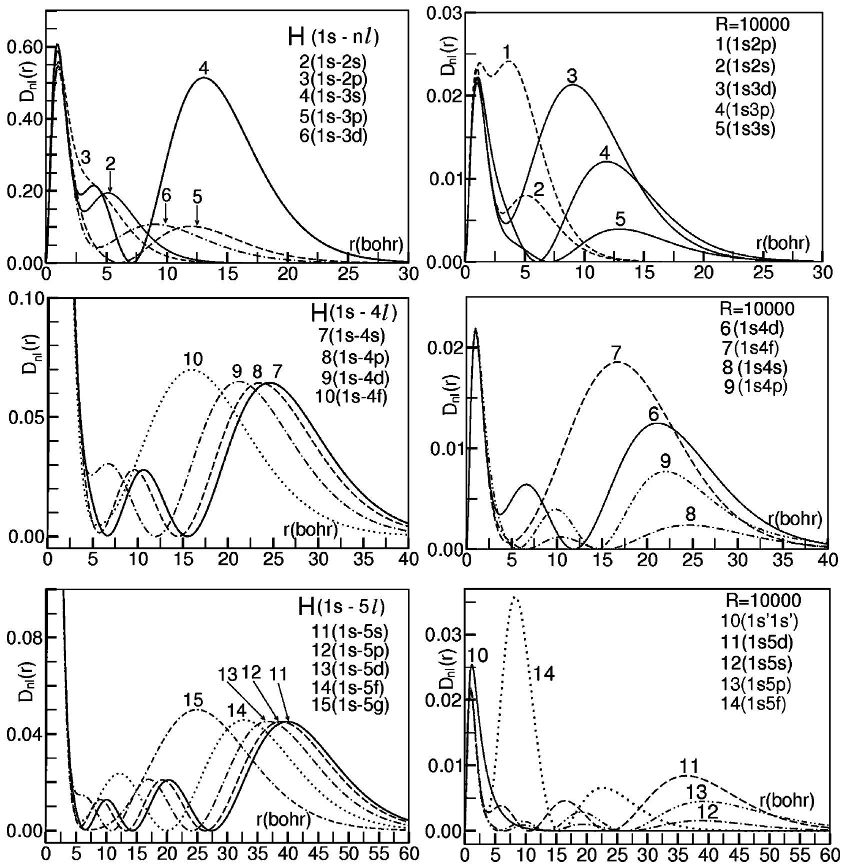

Figure 7. Right: plots of $D_{1s}(r) + D_{nl}(r)$ radial distributions of hydrogenic orbitals. Left: plot of "*state*"(1s,*nl*)(*r*), with n = 1 to 5, for H_2 at the internuclear distance R = 10000 bohr.

The state 9B configuration from dissociation to 10 bohr is (1s4p); from 6.2 to 5.0 bohr it is (1s5*l*) first (1s5f), then (1s5p) and finally (1s5s); from 2.5 bohr to the united atom it becomes (1s7*l*) first (1s7d) until 2.0 bohr then (1s7p); the united atom is He(1s7f).

State 10B dissociates as H^+H^-. From 100 to 10 bohr the configuration is (1s4*l*), starting with (1s4s). At 6.2 bohr it becomes (1s5p); from 5.7 to 5.0 bohr it is (1s6*l*); from 2.5 to 2.0 bohr it is (1s8p) and then switches to (1s7f) until the united atom, which is He(1s7p).

States 11B, 12B, 13B and 14B dissociate as (1s5d), (1s5s), (1s5p) and (1s5f), respectively; the corresponding states at the united atom are He(1s8f), He(1s8p), He(1s9f), and He(1s9p). The radial densities for these states are characterized by many nodes, therefore not easily classifiable.

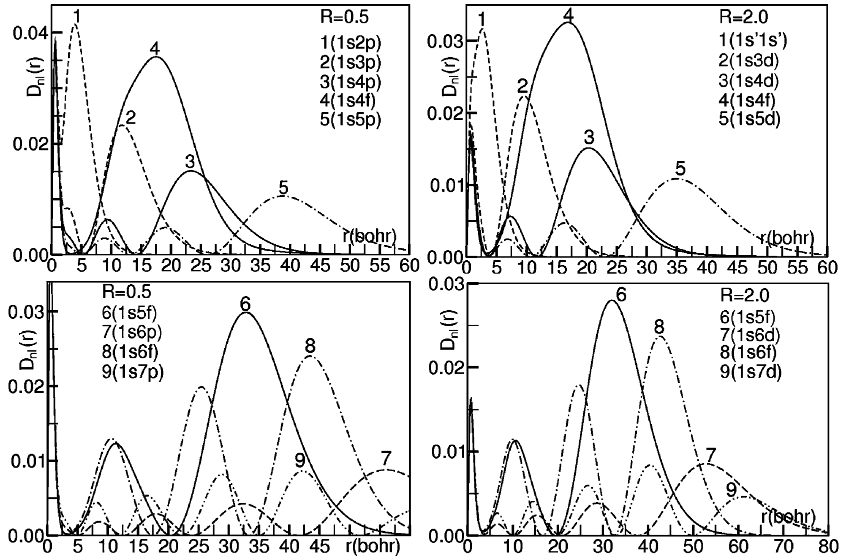

Figure 8. Plots of "*state*"(1s,*nl*)(*r*) for states 1 to 9. Right: at the internuclear distance $R = 0.5$ bohr. Left: at $R = 2.0$ bohr.

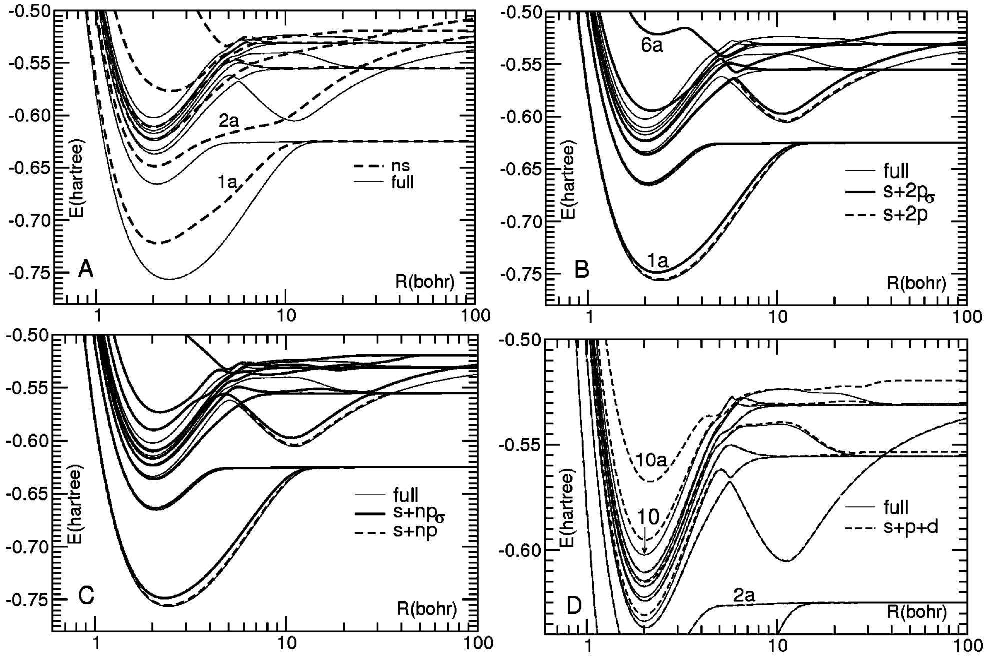

Figure 9. PECs computed with STO subsets (dashed curves) and full STO basis set (thin full curves).

5. Basis Subset Decompositions

The identification of the electronic configurations obtained in the previous section is confirmed by decomposing the STO basis set into subsets with the same *l* value (for example all the *n*s STO, or all the *n*p STO, etc.) These subsets bring specific and characteristic contributions to the total energy of the 1B to *n*B states and thus to the corresponding electronic density. The results of this analysis are summarized in Figures 9 and 10.

The top left panel of Figure 9 reports computations of the B states using only *n*s STO (dashed curves) to be compared with thin lines (full curves) representing the final computations previously reported in Figure 2. With the *n*s subset only the 1B and the 2B state are crudely reproduced, indicating a strong *n*s contribution for these states. The curve 1a and, starting from ~3 bohr until dissociation, the 2a are formed by the 2s functions. The 3s functions generate the first minimum of curve 2a and, starting from 3 bohr until dissociation the two curves 3a and 4a which cross in the region 6−7 bohr. The state crossing at ~5.3 bohr between curves 5a and 6a is generated by the 4s functions. The first cross, between 3a and 4a, is retained in the final PECs, and the second one resolves into a pronounced bump for state 5B. At this level, the dashed PECs for the 3B, 4B and 5B states are clearly incorrectly reproduced, indicating the need of STO of higher *l* values.

Indeed, proceeding to the top right panel, one can see that the combined *n*s and 2p STO subsets are capable of reproducing, although with different accuracy, the states 1B, 2B, 3B, 4B and, only approximately, 5B. The avoided state crossings between curves 3a and 4a and between 5a and 6a are now more evident. Further, from the figure we learn that most of the 2p effect is due to $2p_\sigma$ functions (thick full lines) with limited contribution from the $2p_\pi$ (dashed lines), important only for the 1a and 3a curves. Addition of the full *n*p subset improves the accuracy which is now acceptable for the states 1B, 2B and 3B.

Addition of the *n*d STO subset notably improves the energy for all the states dissociating up to 1s + 4*l*. For the higher states

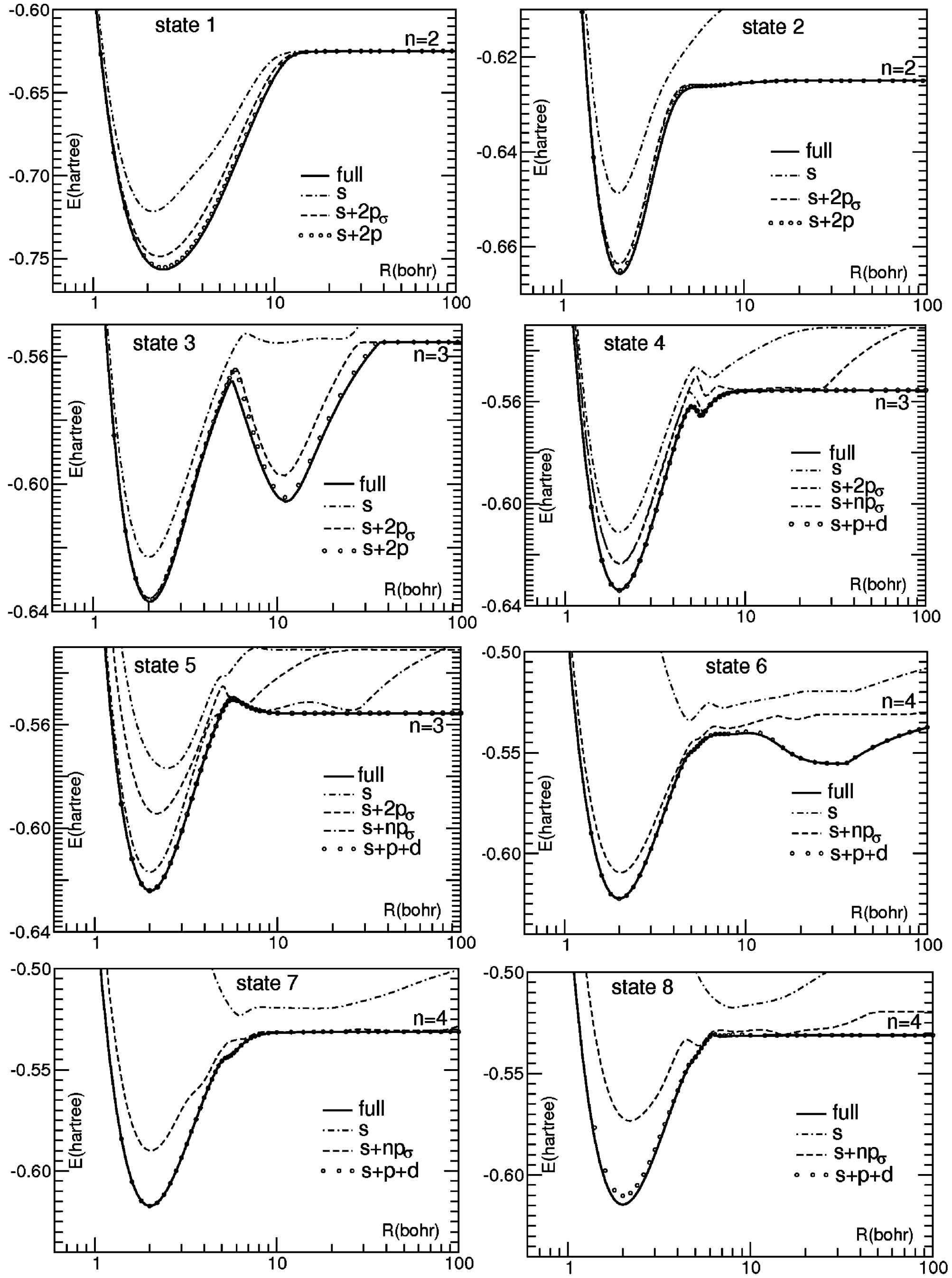

Figure 10. PECs for states 1 to 8 obtained from *n*s STO subsets to full STO basis set.

the representation is poor. These graphs are overcrowded, thus not easily readable, but provide a synthetic and overall summary on the effect of the different subsets of STO, and confirm the density analysis conclusions.

The graphs reported in the panels of Figure 10 confirm clearly and in detail the conclusions above obtained for the states 1B to 8B. From this figure we note that for the 1B, 2B and 3B states large energy improvements are mainly due to $2p_\sigma$ STO. For the state 4B the $3p_\sigma$ is dominant among the np_σ STO; for states 5B to 8B the STO $3p_\sigma$, $4p_\sigma$, and $5p_\sigma$ become dominant. The need of inclusion of the *n*d STO becomes apparent starting from state 5B until state 8B. The need of *n*f STO is clearly noted for state 8B.

This state by state energy decomposition analysis confirms the previous deductions on the main contribution by specific *nl* orbitals for the $^1\Sigma_u^+$ states.

6. Conclusions

The $^1\Sigma_u^+$ state computations reported in this work are performed with extended and optimized STO and GTO basis sets. The energies of the 1B to 6B states are in nice agreement with the accurate computations by Wolniewicz et al.[9] and slightly better than those reported in ref 7.

The evolution of the electronic density is analyzed in detail state by state with the comparative probability density analysis, and by a study of the relative importance of basis subsets. The computations for states 6B to 9B complete for the first time the manifold of states dissociating as H(1s) + H(4*l*). For the state manifold dissociating into H(1s) + H(5*l*) the computations reported are less reliable, due to limitations in the basis sets for high *n* and *l* values; however, we find that these states dissociate correctly and all, but B10, have minima lying just above the $1\sigma_g$ state of the H_2^+ system.

The ionic character of the $^1\Sigma_u^+$ states is quantitatively determined. For states dissociating as (1s*nl*) a rule has been noted: for each $n > 1$ value there is one state which strongly interacts with the H^+H^- system leading to minima with ionic character at larger and larger internuclear separations the higher the value of *n*. This rule, previously found for the $^1\Sigma_g^+$ state, is here extended to the $^1\Sigma_u^+$ states. In both cases, the first state of the (1s5*l*) manifold dissociates as H^+H^-.

Acknowledgment. One of us (G.C.) acknowledges a grant from MIUR-2006030944.

References and Notes

(1) Corongiu, G.; Clementi, E. *J. Chem. Phys.* **2009**, *131*, 034301.
(2) Kolos, W.; Wolniewicz, L. *J. Chem. Phys.* **1965**, *43*, 2429.
(3) Kolos, W.; Wolniewicz, L. *J. Chem. Phys.* **1966**, *45*, 509.
(4) Rothenberg, S.; Davidson, E. R. *J. Chem. Phys.* **1966**, *45*, 2560.
(5) Kolos, W. *J. Mol. Spectrosc.* **1976**, *62*, 429.
(6) Dressler, K.; Wolniewicz, L. *Ber. Bunsen-Ges. Phys. Chem.* **1995**, *99*, 246.
(7) Detmer, T.; Schmelcher, P.; Cederbaum, L. S. *J. Chem. Phys.* **1998**, *109*, 9694.
(8) de Lange, A.; Hogervorst, W.; Ubachs, W.; Wolniewicz, L. *Phys. Rev. Lett.* **2001**, *86*, 2988.
(9) Staszewska, G.; Wolniewicz, L. *J. Mol. Spectrosc.* **2002**, *212*, 208.
(10) Huber, K. P.; Herzberg, G. *Molecular Spectra and Molecular Structure IV. Constants of Diatomic Molecules*; Van Nostrand Reinhold: New York, 1979.
(11) Ishikawa, A.; Nakashima, H.; Nakatsuji, H. *J. Chem. Phys.* **2008**, *128*, 124103.
(12) Vieitez, M. O.; Ivanov, T. I.; Reinhold, E.; de Lange, C. A.; Ubachs, W. *Phys. Rev. Lett.* **2008**, *101*, 163001.
(13) Slater, J. C. *J. Chem. Phys.* **1951**, *19*, 220.
(14) Mulliken, R. S. *J. Am. Chem. Soc.* **1966**, *88*, 1849.
(15) Koelemeij, J. C. J.; de Lange, A.; Ubachs, W. *Chem. Phys.* **2003**, *287*, 349.
(16) Reinholds, E.; Ubachs, W. *Mol. Phys.* **2005**, *103*, 1329.
(17) Pauling, L.; Wilson, E. B. *Introduction to Quantum Mechanics*; McGraw-Hill Book Company: New York, 1935.
(18) Moore, C. E. *Atomic Energy Levels, Vol. 1, NBS Circular 467*; U.S. Government Printing Office: Washington, DC, Dec 1971.

JP9049395